Redox Biology 63 (2023) 102739

Contents lists available at ScienceDirect

Redox Biology

journal homepage: www.elsevier.com/locate/redox

ROS-Drp1-mediated mitochondria fission contributes to hippocampal HT22 cell apoptosis induced by silver nanoparticles

Xiaoru Chang, Shuyan Niu, Mengting Shang, Jiangyan Li, Menghao Guo, Wenli Zhang, Zuoyi Sun, Yunjing Li, Rui Zhang, Xin Shen, Meng Tang, Yuying Xue *

Key Laboratory of Environmental Medicine and Engineering, Ministry of Education, School of Public Health, Southeast University, Nanjing, 210009, China

ARTICLE INFO

Keywords:
Silver nanoparticles
Neurotoxicity
Mitochondrial fission
Drp1
Apoptosis

ABSTRACT

Silver nanoparticles (AgNPs) have widely used in industrial and medical applications for their excellent antibacterial activities. AgNPs can penetrate into the brain and cause neuronal death, but limited evidence focused on toxic effects and mechanic study in hippocampal neuron. This study aimed to investigate the molecular mechanisms of mitochondrial damage and apoptosis in mouse hippocampal HT22 cells and further to explore role of reactive oxygen species (ROS) and GTPase dynamin-related protein 1 (Drp1) in AgNPs-induced neurotoxicity. Our results showed that acute exposure to AgNPs at low doses (2–8 μg/mL) increased ROS generation, decreased mitochondrial membrane potential (MMP) and ATP synthesis in HT22 cells. In addition, AgNPs promoted mitochondrial fragmentation and mitochondria-dependent apoptosis via excessive mitochondrial fission/fusion by 8 μg/mL AgNPs treatment for 24 h. The mechanism was involved in increased protein expression of Drp1, mitochondrial fission protein 1 (Fis1), mitofusin 1/2 (Mfn1/2) and inhibited optic atrophy 1 (OPA1), and mainly mediated by phosphorylation of Drp1 Ser616. The AgNPs-induced mitochondrial impairment and apoptosis was mainly due to their particle-specific effect rather than silver ions release. Furthermore Drp1-mediated mitochondrial fission contributed to mitochondria-dependent apoptosis induced by AgNPs, all aforementioned changes were significantly rescued by N-acetyl-L-cysteine (NAC) and Mdivi-1 except for OPA1 protein expression. Hence, our results provide a novel neurotoxic mechanism to AgNPs-induced neurotoxicity and revealed that the mechanism of mitochondria-dependent apoptosis in HT22 cells was mediated by excessive activation of ROS-Drp1-mitochondrial fission axis. These findings can deepen current evidences on neurotoxicological evaluation of AgNPs and aid in guiding their proper applications in different areas, especially in biomedical use.

1. Introduction

Silver nanoparticles (AgNPs) exhibit distinctive physical, chemical and biological properties that make them suitable for disease therapeutics, medical imaging and molecular diagnostics [1]. For these applications, AgNPs unavoidably enter the human body distribute in the central nervous system (CNS), leading to neurotoxicity and consequently threatening human health [2]. Despite numerous publications on the neurotoxicity of various AgNPs *in vitro* and *in vivo* [2,3], details of AgNP-induced neurotoxicity need to be elucidated. Mitochondria are major target of AgNPs-induced cytotoxicity [4]. The involved changes included mitochondrial membrane potential (MMP) loss, oxidative phosphorylation inhibition, calcium dynamics disruption and reactive oxygen species (ROS) elevation, eventually caused mitochondria-dependent apoptosis [4,5]. AgNPs were reported to induce apoptosis in HT22 cells, which is mitochondria-dependent [6]. But involved molecular mechanisms targeting mitochondria remain unclear in the AgNPs-induced neurotoxicity. As hippocampal neuron was vulnerable to AgNPs, more neurotoxic effects should be deeply understood.

Mitochondrial fission/fusion are the process that mitochondria undergo coordinated dynamic cycles. The events refer to mitochondria dynamics that closely related with mitochondrial function to maintain energy metabolism, calcium homeostasis and redox balance and cell fate [7]. Mitofusin 1 (Mfn1), Mitofusin 1 (Mfn2) and optic atrophy 1 (OPA1) are fusion proteins that control mitochondrial fusion. Fission is orchestrated by mitochondrial fission protein 1 (Fis1), which recruits cytosolic GTPase dynamin-related protein 1 (Drp1) to cleave mitochondria [8].

* Corresponding author.
E-mail address: yyxue@seu.edu.cn (Y. Xue).

https://doi.org/10.1016/j.redox.2023.102739
Received 11 April 2023; Received in revised form 28 April 2023; Accepted 9 May 2023
Available online 9 May 2023

Drp1 Ser616 activation driven excessive mitochondrial fission exacerbates oxidative stress and apoptosis [9–13], the expression of Drp1 is various in different nanoparticles. Target biomarker of mitochondrial fission/fusion in AgNPs-induced neurotoxicity is also uncertain. In our previous study, we found AgNPs promoted excessive ROS generation, decreased ATP production and MMP dissipation, indicating mitochondria dysfunction. In human hepatocellular carcinoma cells (HepG2 cells), AgNPs also induced mitochondrial fission and apoptosis through Drp1 translocation to mitochondria [13]. However, mitochondrial fission may be a causative or protective element, role of AgNPs-induced mitochondrial fission in neuronal cell fate needs to be elucidated. Additionally, it is not clear whether change in the Drp1-driven mitochondrial fission equilibrium occurs secondary to oxidative stress in hippocampal neurons.

Our previous study found that AgNPs accumulated in mouse hippocampal neurons and induced neuronal mitochondrial damage [14]. So hippocampal HT22 cells was used in this study, because it is sensitive model for oxidative stress due to the lack of ionotropic glutamate receptors [15]. This study aimed to investigate role of mitochondrial fission in cell fate and explore the regulatory relationship between mitochondrial fission and oxidative stress in the neurotoxicity induced by AgNPs. Our findings will provide a better understanding on the mechanism of AgNPs-induced neurotoxicity *in vitro* and facilitate safer biomedical application of AgNPs.

2. Materials and methods

2.1. Characterizations of AgNPs

Polyvinylpyrrolidone (PVP)-coated AgNPs were purchased from Shanghai Huzheng Nano Technology Co., Ltd. (Shanghai, China). The AgNPs morphology was characterized by transmission electron microscope (TEM, JEOL, Japan). The dynamic light scattering of AgNPs in cell culture medium was measured using Malvern Zetasizer Nano-ZS90 instrument (Malvern Instrument Ltd., UK). The maximum absorbance peak of AgNPs was analyzed by ultraviolet visible (UV–vis) spectroscopy.

2.2. Cell culture and cell viability determination

HT22 cells (Shanghai Institute of Cell Biology, China) were cultured in Dulbecco's modified Eagle's medium (DMEM) (Gibco, USA) supplemented with 10% fetal bovine serum (FBS) and 1% penicillin-streptomycin antibiotics (Gibco, USA) in an incubator with 5% CO_2 in 37 °C. HT22 cells (1×10^3 cells/well) were seeded in a 96-well culture plate overnight and exposed to AgNPs (0–12 μg/mL) or $AgNO_3$ (0–1.2 μg/mL) for 24 h. After the treatment, the cells were added 10 μL cell counting kit 8 (CCK8, Meilunbio, China) solution, incubated at 37 °C for 1 h and measured absorbance at 450 nm by microplate reader. The selected AgNPs exposure dose was according to the CCK8 assay. In addition, HT22 cells were also pretreated with 5 mM antioxidant N-acetyl-L-cysteine (NAC) or 5 μM Drp1 inhibitor Mdivi-1 for 2 h, and exposure to AgNPs (8 μg/mL) for 24 h in the subsequent assay.

2.3. Cellular uptake of AgNPs

After AgNPs exposure, HT22 cells (30×10^5 cells/well) were digested with 3 mL 65% HNO_3 and 2 mL 30% H_2O_2. After the pretreatment of the cells, silver content in HT22 cells were detected by inductively coupled plasma mass spectrometry (ICP-MS). In addition, particles uptake of HT22 cells was analyzed by flow cytometry (BD, USA). Free Ag^+ released from AgNPs was detected by ultrafiltration combined with ultracentrifugation [16]. According to the result of cellular uptake for AgNPs, comparable silver content of $AgNO_3$ was used to subsequent experiment. The control is untreated cells and the Ag^+ control is $AgNO_3$-treated cells that has comparable silver content with 8 μg/mL AgNPs.

2.4. Ultrastructural observation

After exposure to AgNPs/$AgNO_3$, HT22 cells were fixed in 2.5% glutaraldehyde overnight. The mitochondrial morphology was examined using TEM, which involved in three different parameters: mitochondrial number, aspect ratio (AR, mitochondrial major axes/minor axes) and form factor (FF, perimeter 2/4π•area) referred to their branching degree [7]. AgNPs distribution was detected by TEM.

2.5. Analyses of mitochondrial morphology

HT22 cells were treated for 40 min with 50 nM MitoTracker Red CMXRos (Yeasen, China), then mitochondrial morphology was observed by confocal laser microscope (Olympus, Japan; FV1000).

2.6. Intracellular ROS measurement

DCFH-DA staining (Beyotime, China) was used to determine ROS. Briefly, the harvested cells were stained with 2.5 μM DCFH-DA for 30 min, and washed twice with PBS. After washing, 1×10^5 cells were quantified by samples, and ROS level was measured by flow cytometry (BD, USA). Cell Number was chosen according to manufacturer's instructions.

2.7. Mitochondrial membrane potential measurement

MMP ΔΨm was measured by JC-1 fluorescent probe (Beyotime, China). Fluorescence intensity of the HT22 cells was measured by fluorescence microscopy (ZEISS, Germany), after 30 min at 37 °C using 1:200 JC-1 working buffer.

2.8. ATP quantification

Lysates obtained from the treatment were added to HT22 cells, centrifuged at 12,000 g for 10 min at 4 °C, and the ATP detection solution (Beyotime, China) was added according to the manufacturers' instructions. Measurements were performed using a Luminescence microplate reader (LB942, Berthold Technologies, Germany).

2.9. Apoptosis measurement

The apoptotic status of HT22 cells was detected using an annexin-V-FITC/PI labeling method according to the manufacturer (BD, USA). In this study, 10×10^5 cells were collected for staining with 5 μL Annexin-V FITC and PI for 15 min, the apoptotic rate was analyzed by flow cytometry (BD, USA).

2.10. Immunofluorescence

HT22 cells were fixated in 4% paraformaldehyde, permeabilized, and blocked using PBS containing 5% BSA and 0.5% TritonX-100. Primary antibody anti-Drp1 (1:100, ABclonal, China) was incubated overnight at 4 °C with cells. The cells were then incubated with Alexa Fluor 488 conjugated anti-rabbit IgG secondary antibody (1:200, Beyotime, China) for 1 h, followed by staining with DAPI (Beyotime, China). The images were visualized by confocal laser microscopy (Olympus, FV1000, Japan).

2.11. Western blot

After lysing on ice for 30 min with RIPA containing 1% phenylmethanesulfonyl fluoride (PMSF, Beyotime, China), cells were centrifuged 12,000 *g* to collect supernatant (at 4 °C for 15 min). The supernatant was collected to quantify protein content by BCA kit

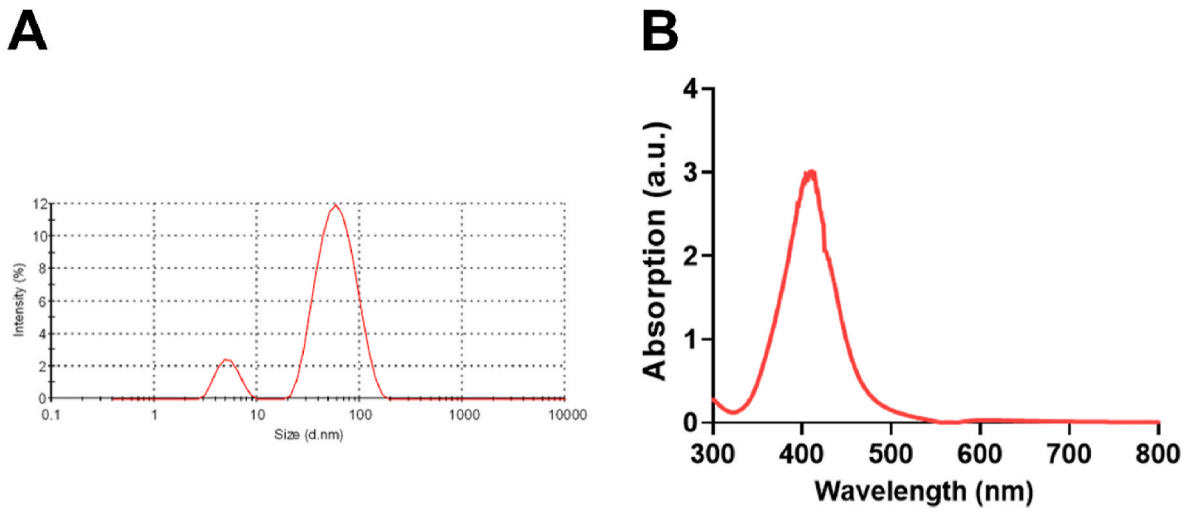

Fig. 1. Characterizations of AgNPs. (A) The hydrodynamic sizes of the AgNPs in cell culture medium (DMEM containing 10% FBS). (B) UV–vis spectrum of AgNPs in cell culture medium.

(Thermo, USA). SDS-PAGE was used to separate the total protein, then transferred to an Immobilon™ PVDF membrane (Millipore, USA) was applied for 90 min at 220 mV. The blot was blocked with TBST (0.1% Tween-20 in Tris buffered saline) containing 5% skim milk powder for 2 h, and incubated with primary antibodies: Drp1, Fis1, Mfn1, Mfn2, OPA1, Caspase-3, Bax, Bcl-2 (their dilution ratio was all 1:1000, Abclonal, China), p-Drp1 S616 (1:1000, Affinity, USA) overnight at 4 °C. After washing three times with TBST, the PVDF membrane was incubated with horseradish peroxidase-coupled (HRP) Goat Anti-Rabbit IgG secondary antibody (1:5000, Abclonal, China) for 1 h. The image collection was performed using BeyoECL plus Western blotting detection system.

2.12. Statistical analysis

The significance of the results was tested by one-way analysis of variance (ANOVA) among control and treated group, least significant difference (LSD) test was performed for statistical significance test by SPSS 22.0 (Chicago, USA). $P < 0.05$ was considered statistically significant.

3. Results

3.1. Characterization of AgNPs

The average diameter of AgNPs was 23.53 ± 4.79 nm (Fig. S1), as reported in our previous study [14]. In the cell culture medium, the average hydrated diameter of AgNPs was 65.80 ± 1.89 nm, the Zeta potential of AgNPs was −2.58 ± 0.78 mV (Fig. 1A), specific absorption peak of AgNPs was 400–420 nm (Fig. 1B).

3.2. Cytotoxicity of AgNPs in HT22 cells

HT22 cells exposed AgNPs exhibited cytotoxicity with increasing concentrations and duration of exposure (Fig. 2A). AgNPs hardly reduced cell viabilities for 12 h exposure in all exposure concentrations (2–12 μg/mL). After AgNPs exposure for 24 h, cell viability was reduced to <50% at dose of 10–12 μg/mL (Fig. 2A). Based on the concentration-response curve, the inhibitory concentration (IC) at which 50% reduction in cell viability occurs was calculated. The IC50 value of AgNPs exposure for 24 h was 10.8 μg/mL, and for the $AgNO_3$, it was 0.62 μg/mL (Fig. 2B). 2–8 μg/mL exposure doses and 24 h exposure-time of AgNPs was selected for further studies.

3.3. Distribution and uptake of AgNPs in HT22 cells

Cellular distribution of AgNPs in HT22 cells after 24 h exposure was shown in Fig. 2C. AgNPs (8 μg/mL) was observed in the cytoplasm of HT22 cells (Fig. 2C). The silver internalization rate of HT22 cells exposed to AgNPs (2–8 μg/mL) was measured using ICP-MS to quantitatively analyze the cellular uptake. The silver content was 0.095 ng/10^5 cells (Fig. 2D), and intracellular Ag^+ content was 0.003 ng/10^5 cells (Fig. 2E) in HT22 cells treated by AgNPs (8 μg/mL) for 24 h. The results indicated that the Ag^+ release from AgNPs (8 μg/mL) in the HT22 cells was 3.16%. And the Ag^+ content was 0.01 ng/mL in cell culture medium (Fig. 2F). The theoretical silver content of AgNPs-PVP is 20%, so the theoretical Ag^+ content was 0.1 μg/mL released from 8 μg/mL AgNPs. Based on the results of Ag^+ release and cell viability, we chose 8 μg/mL AgNPs and 0.1 μg/mL $AgNO_3$ in this study. Intensity of side scatter light (SSC) could reflect intracellular AgNPs concentrations detected by flow cytometry. Compared with the control group, AgNPs (2–8 μg/mL) increased SSC of HT22 cells in a dose-dependent manner (Fig. 2G). Despite SSC was changed in silver ion-treated group compared to the control cells, the change level is lower compared with AgNPs-treated groups (Fig. 2H).

3.4. AgNPs disrupted mitochondrial morphology and function in HT22 cells

Changes of mitochondrial structure and morphology were observed in AgNPs (8 μg/mL) groups. We found a remarkably scattered distribution, mitochondria exhibit fragmented and punctate morphology in AgNPs-treatment (8 μg/mL) group (Fig. 3A). Fragmented mitochondria were also observed by TEM, the number of fragmented mitochondria in HT22 cells was increased by approximately 3.76 folds (Fig. 3B). After AgNPs exposure (8 μg/mL), AR was decreased by approximately 40.58%, and FF was increased by approximately 1.9 folds respectively (Fig. 3C). But it was not changed in $AgNO_3$ group. After 8 μg/mL AgNPs exposure, the mitochondrial network looked disrupted and mitochondria appeared as small fragmented punctiform structures (Fig. 3D). These results suggested that the mitochondria were rounder and more fragmented in AgNPs-treated cells rather than Ag^+ in HT22 cells.

Normal structure is vital to maintain mitochondrial functions. We further detected AgNPs-induced mitochondrial functions (including intracellular levels of ROS, ATP and MMP) in HT22 cells. Compared with the control group, intracellular ROS levels were increased approximately 2.06 and 3.82 folds by 4–8 μg/mL AgNPs respectively (Fig. 3E and F). MMP was measured by the JC-1 assay, cells in green color

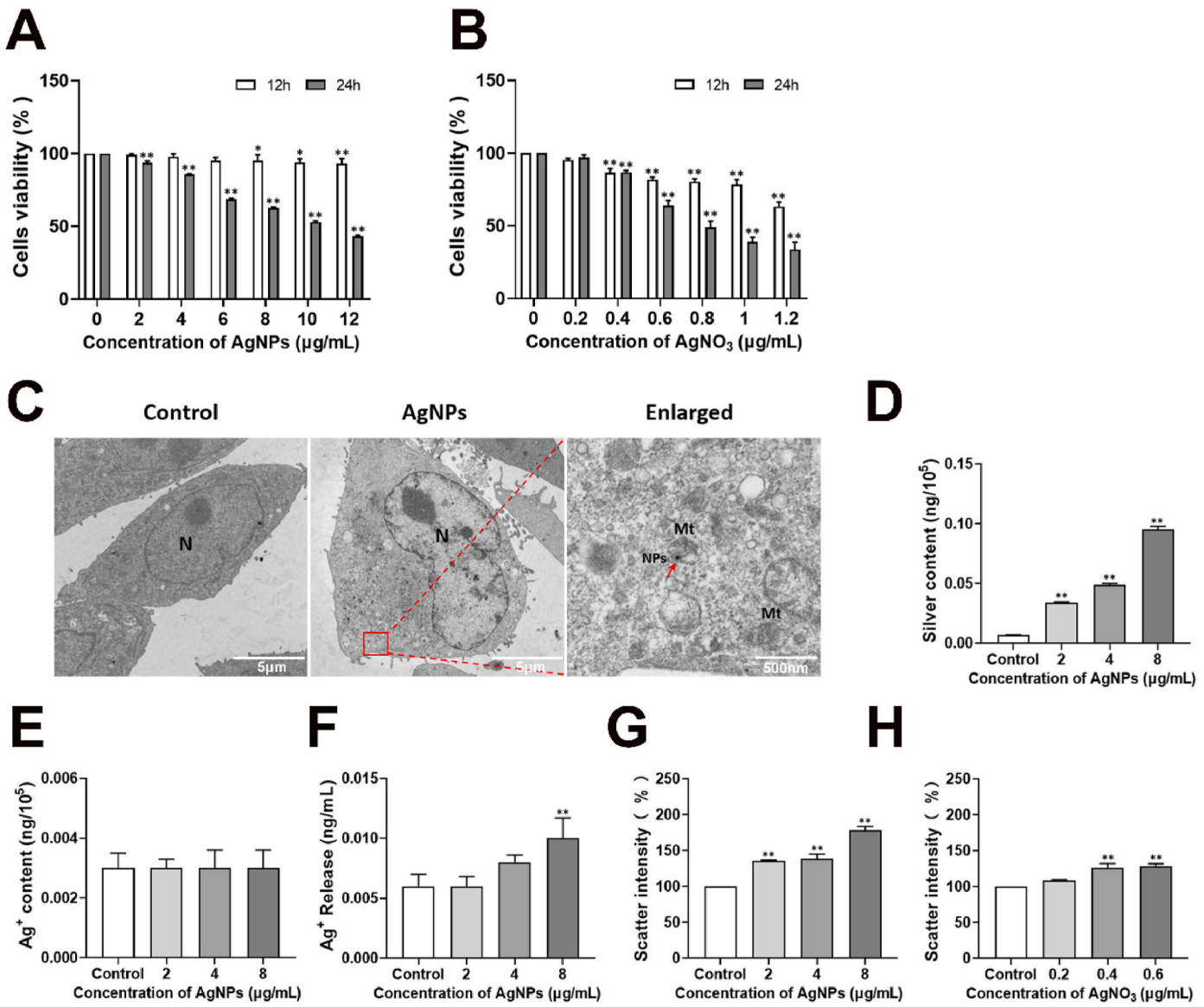

Fig. 2. Cytotoxicity, distribution and uptake of AgNPs in HT22 cells. (A–B) Cytotoxicity of HT22 cells, after AgNPs (0–12 μg/mL) or $AgNO_3$ (0–1.2 μg/mL) exposure for 24 h; (C) Cellular distribution of AgNPs in HT22 cells, after AgNPs (8 μg/mL) exposure for 24 h, the red arrow indicates engulfed AgNPs; (D–F) Silver content (D), Intracellular Ag^+ content (E) and released Ag^+ content in cell culture medium (F) in HT22 cells, after AgNPs (0–8 μg/mL) exposure for 24 h; (G–H) Dose-dependent scattering intensities as a percentage of control for HT22 cells treated with AgNPs (0–8 μg/mL) or Ag^+ (0–0.6 μg/mL) for 24 h. NPs: nanoparticles; Mt: mitochondria. Data are expressed as mean ± SD from three independent experiments. $*p < 0.05$, $**p < 0.01$ when compared with the control. (For interpretation of the references to color in this figure legend, the reader is referred to the Web version of this article.)

suggested decreased MMP, while those in red color indicated high MMP. As shown in Fig. 3G and H, compared with the control, AgNPs (2–8 μg/mL) decreased MMP in HT22 cells (the JC-1 ratio of monomers/aggregate were increased 1.56, 1.96, 2.43 folds respectively). ATP levels of HT22 cells was decreased 32.6% by AgNPs (8 μg/mL) compared with control group (Fig. 3I). However, the mitochondrial functions including ROS, MMP and ATP were not changed by $AgNO_3$ (Fig. S2). These results suggested the onset of mitochondrial dysfunction.

3.5. AgNPs induced disruption of the mitochondrial dynamics in HT22 cells

Protein expression of Drp1, p-Drp1, Fis1, Mfn1 and Mfn2 was increased by AgNPs (2–8 μg/mL) and OPA1 protein expression was decreased by AgNPs only at 8 μg/mL (Fig. 4A–C). Specifically, after AgNPs (8 μg/mL) exposure, Drp1 in the cytoplasm translocated Drp1 to mitochondria (Fig. 4A), p-Drp1 protein expression was increased approximately 2.27 folds by 8 μg/mL AgNPs exposure (Fig. 4B and C). These results indicate that AgNPs phosphorylates Drp1 at serine 616 site, triggers Drp1 translocation from the cytoplasm to mitochondria, eventually induces mitochondrial fragmentation and dysfunction.

3.6. AgNPs induced mitochondria-dependent apoptosis in HT22 cells

The apoptotic rate of HT22 cells was significantly increased by AgNPs (4–8 μg/mL) (Fig. 5A and B), but not changed in $AgNO_3$ (0.2 μg/mL) group (Fig. 5C and D), indicating AgNPs-induced apoptosis was involved in inherent nanoscale effects of AgNPs (particle special) rather than Ag^+ release in HT22 cells. AgNPs (2–8 μg/mL) exposure increased the Bax, cytochrome C (Cyt-C) protein expression and decreased Bcl-2 protein expression (Fig. 5E and F). Furthermore, AgNPs (4–8 μg/mL) increased the protein expressions of pro-caspase-3 and cleaved Caspase-3 (Fig. 5E and F). These results suggested that AgNPs-induced apoptosis was mitochondria-dependent.

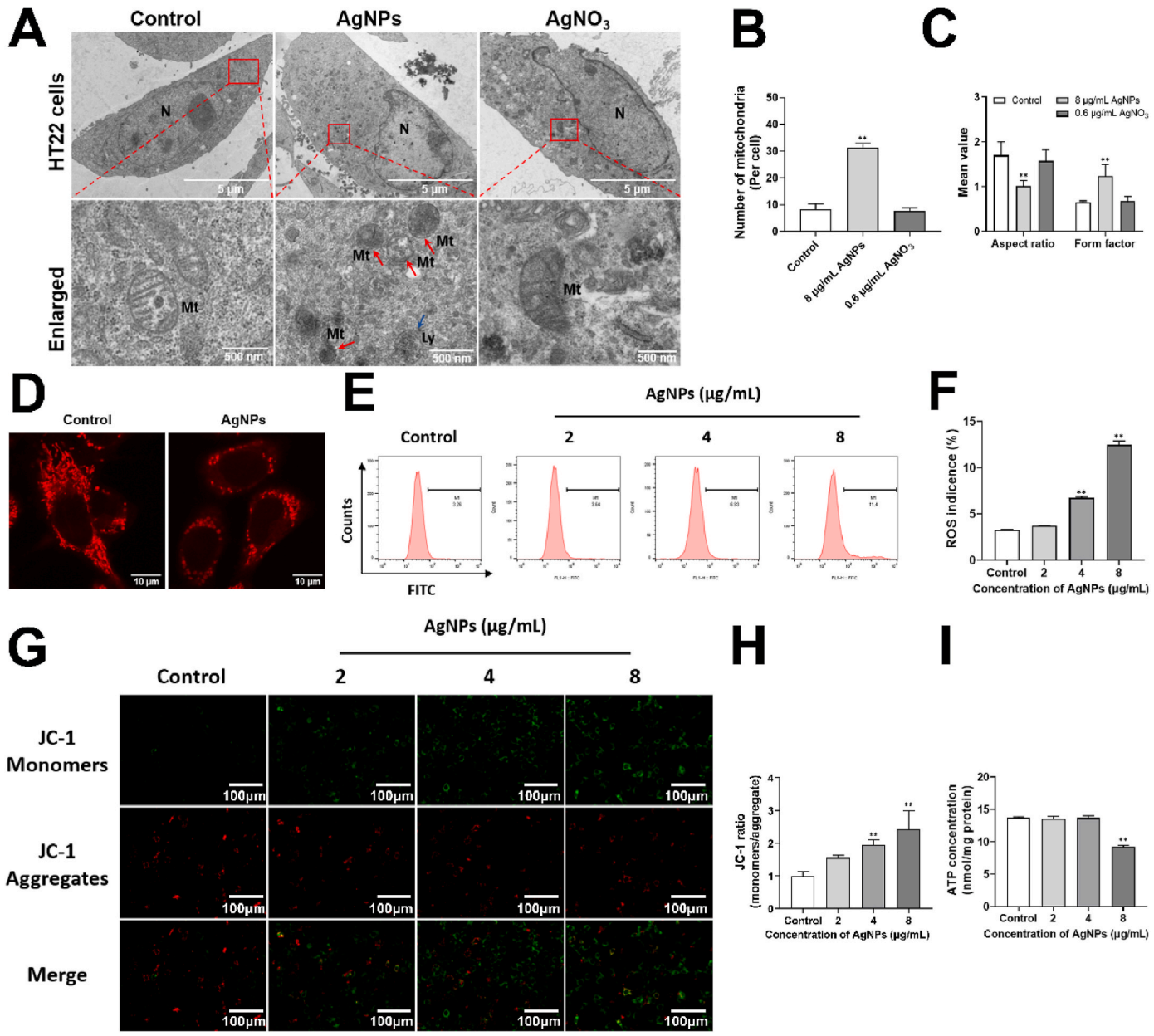

Fig. 3. AgNPs disrupted mitochondrial morphology and function in HT22 cells. (A–C) Alterations of mitochondrial morphology (A), mitochondrial number (B), mitochondrial AR and FF parameter (C) in HT22 cells, after AgNPs (8 μg/mL) or $AgNO_3$ (0.6 μg/mL) exposure for 24 h, the red arrow indicates mitochondrial fission and fragmentation, the yellow arrow indicates mitochondrial fusion; (D) Alterations of mitochondrial structure and Mitotracker fluorescence in HT22 cells, after AgNPs (8 μg/mL) exposure for 24 h; (E–F) Intracellular ROS levels, (G–H) MMP changes, (I) ATP content in HT22 cells, after AgNPs (0–8 μg/mL) exposure for 24 h. AR: aspect ratio (ratio between major and minor axes of an ellipse); FF: form factor (perimeter^2/4π•area; degree of branching). Data are expressed as mean ± SD from three independent experiments. *$p < 0.05$, **$p < 0.01$ when compared with the control. (For interpretation of the references to color in this figure legend, the reader is referred to the Web version of this article.)

3.7. ROS promoted mitochondrial fragmentation and mitochondrial dysfunction induced by AgNPs in HT22 cells

To explore role of ROS in mitochondrial damage, mitochondrial changes was detected in NAC-treated HT22 cells. Mitotracker fluorescence was decreased by AgNPs (8 μg/mL), which was reversed by NAC (Fig. 6A). Intracellular ROS was increased by AgNPs (8 μg/mL), which was significantly reversed by NAC (Fig. 6B and C). The MMP and ATP content was reduced by AgNPs (8 μg/mL), and partially restored by NAC (Fig. 6D–F). These results suggested that ROS promoted mitochondrial damage.

3.8. ROS promoted mitochondrial fission/fusion and enhanced mitochondria-dependent apoptosis induced by AgNPs in HT22 cells

To further explore role of ROS in the mitochondrial dynamic and mitochondria-dependent apoptosis, biomarkers of mitochondrial fission/fusion and apoptosis were detected in HT22 cells treated by AgNPs and NAC. The results showed that AgNPs (8 μg/mL) increased Drp1, p-Drp1 S616, Fis1, Mfn1 and Mfn2 expression, and decreased OPA1 expression significantly, which was reversed by NAC except for OPA1 expression in HT22 cells (Fig. 7A–C). Especially, the mitochondrial translocation of Drp1 was induced by AgNPs (8 μg/mL) and it was not occurred in NAC-pretreated group (Fig. 7A). Our present study further showed the increased apoptotic ratio (Fig. 7D and E), protein

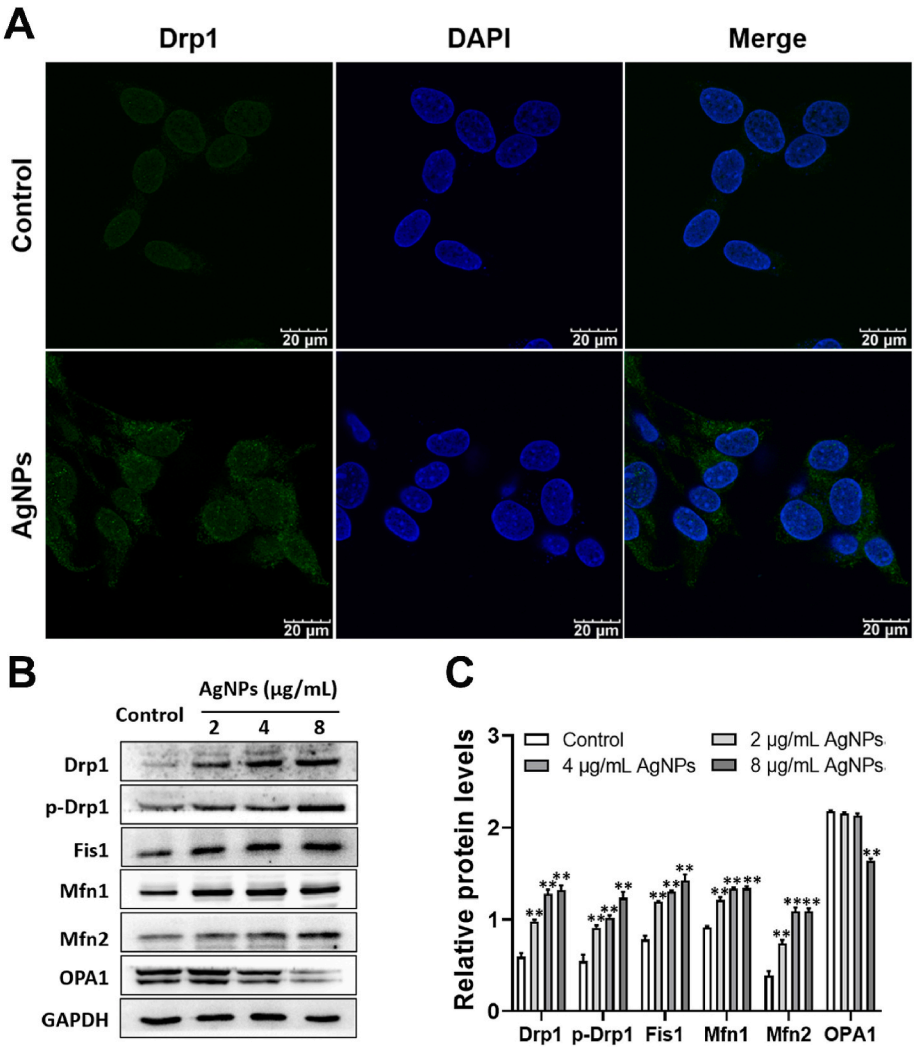

Fig. 4. AgNPs induced disruption of the mitochondrial dynamics in HT22 cells. (A) Immunofluorescence of Drp1in HT22 cells exposed to AgNPs (8 μg/mL) for 24 h; (B–C) Western blot for protein expression of Drp1, p-Drp1, Fis1, Mfn1, Mfn2, OPA1 in HT22 cells, after AgNPs (0–8 μg/mL) exposure for 24 h. Data are expressed as mean ± SD from three independent experiments. $*p < 0.05$, $**p < 0.01$ when compared with the control.

expression of Bax, Cyt-C and caspase-3, decreased Bcl-2 protein expression of HT22 cells induced by 8 μg/mL AgNPs (Fig. 7F and G). NAC pretreatment significantly inhibited the apoptosis and protein expression of those biomarkers (Fig. 7D–G). These results suggested that ROS promote mitochondrial fission/fusion and enhance mitochondria-dependent apoptosis induced by AgNPs in HT22 cells.

3.9. Role of Drp1 on mitochondrial fragmentation and mitochondrial dysfunction induced by AgNPs in HT22 cells

To explore role of Drp1 on mitochondrial fragmentation and the relationship between Drp1 and ROS, we pretreated HT22 cells with Drp1 inhibitor Mdivi-1 (5 μM) for 2 h, and exposed to AgNPs (8 μg/mL) for 24 h. The results showed that mitochondrial fragmentation was increased by AgNPs (8 μg/mL), while it was reduced by Mdivi-1 pretreatment (Fig. 8A). AgNPs increased the ROS level and reduced the MMP and ATP content, the Mdivi-1 rescued the MMP and ATP decline (Fig. 8B–F) while not decrease the intercellular ROS level (Fig. 8B and C). These results indicated Drp1 is the downstream target of ROS in AgNPs-induced neurotoxicity in HT22 cells.

3.10. Role of Drp1-mediated mitochondrial fission on apoptosis induced by AgNPs in HT22 cells

To elucidate role of Drp1-mediated mitochondrial fission on apoptosis induced by AgNPs, biomarkers involved in mitochondrial dynamics and mitochondria-dependent apoptosis were determined by Mdivi-1 pretreatment. The results showed that Mdivi-1 decreased the expression of Drp1, p-Drp1 S616, Fis1, Mfn1 and Mfn2, increased the OPA1 expression (Fig. 9A–C). Furthermore, Mdivi-1 pretreatment inhibited the AgNPs-induced Drp1 translocation from cytoplasm to mitochondria (Fig. 9A). The results indicated that Drp1 inhibition rescued excessive mitochondrial fission caused by AgNPs. AgNPs-promoted apoptosis, Bax, Cyt-C and caspase-3 expression were decreased by Mdivi-1 pretreatment, but it didn't reverse the decreased Bcl-2 expression induced by AgNPs (Fig. 9D–G). These results suggested that inhibition of Drp-1-mediated mitochondrial fission could rescue the mitochondria-dependent apoptosis caused by AgNPs.

4. Discussion

With increased AgNPs applications in the industrial market and biomedical products, public concern is rising regarding the potential human and environmental health implications of AgNPs [2].

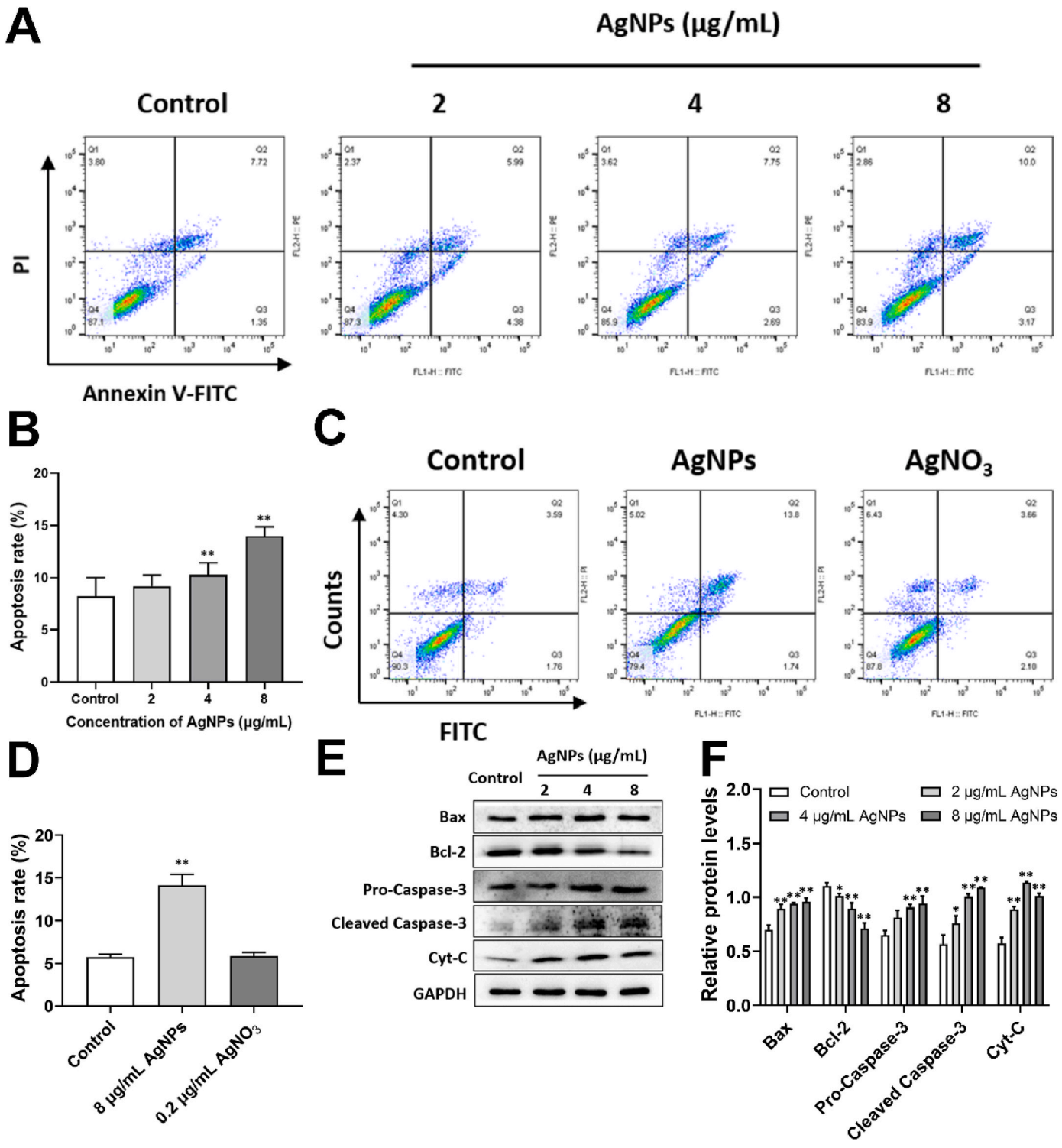

Fig. 5. AgNPs induced mitochondria-dependent apoptosis in HT22 cells. (A–D) Apoptosis rate of HT22 cells, after AgNPs (0–8 μg/mL) or $AgNO_3$ (0.2 μg/mL) exposure for 24 h; (E–F) Western blot for protein expression of Bax, Bcl-2, Caspase-3, Cyt-C in HT22 cells, after AgNPs (0–8 μg/mL) exposure for 24 h. Data are expressed as mean ± SD from three independent experiments. $^{*}p < 0.05$, $^{**}p < 0.01$ when compared with the control.

Neurotoxicity of AgNPs has been reported *in vitro* and *in vivo*, the mechanism is correlated with the mitochondrial damage [3]. Mitochondrial fission/fusion and movement are the basic mechanisms for maintaining mitochondrial morphology. Numerous studies have been investigated the mitochondrial toxicity of nanomaterials, including AgNPs [17]. However, few of them focused on neurotoxicity of nanoparticles. As the brain is vulnerable to AgNPs accumulation, neurotoxic effects and detail mechanisms should be elucidated. Our study revealed that AgNPs induced apoptosis by targeting mitochondria, which involved in oxidative stress and disturbance of mitochondrial dynamic. It was driven by excessive mitochondrial fission via ROS-Drp1-mitochodrial fission axis.

Cytotoxicity is a pivotal element in assessing the prospects of biomedical applications of AgNPs. HT22 cells have already been studied and validated as a sensitive model in the neurotoxicology research field. Our results showed that AgNPs (2–12 μg/mL for 24 h) reduced HT22

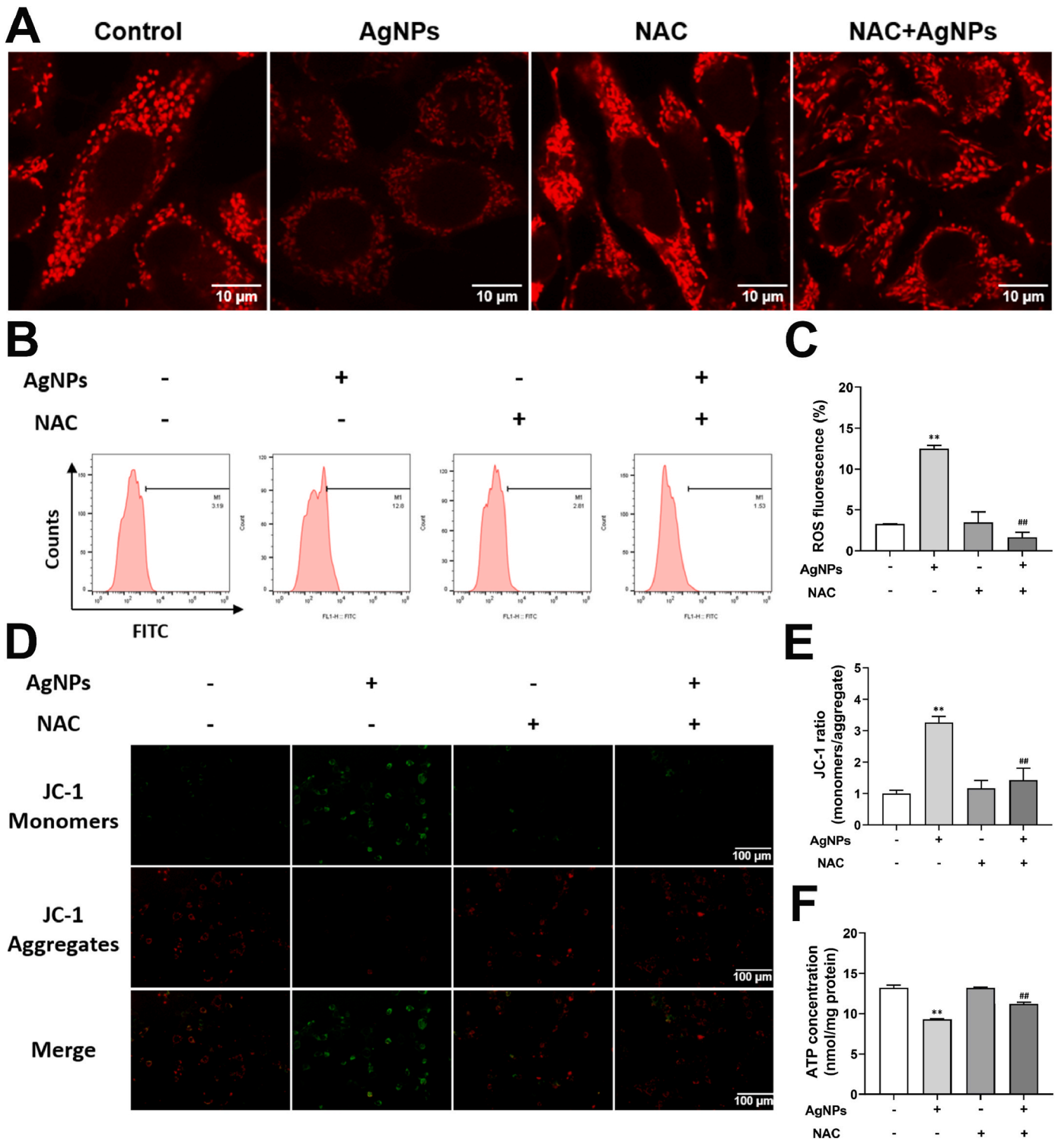

Fig. 6. ROS promoted mitochondrial fragmentation and mitochondrial dysfunction induced by AgNPs in HT22 cells. HT22 cells were pretreated with/without NAC (5 mM) 2 h before exposure to 8 μg/mL AgNPs for 24 h. (A) Alteration of Mitotracker fluorescence in HT22 cells; (B–C) Intracellular ROS levels in HT22 cells; (D–E) MMP changes in HT22 cells; (F) ATP content in HT22 cells. Data are expressed as mean ± SD from three independent experiments. $^{*}p < 0.05$, $^{**}p < 0.01$ when compared with the control. $^{\#}p < 0.05$, $^{\#\#}p < 0.01$ when compared with the AgNPs (8 μg/mL) group.

cells viability in a dose-dependent manner. Cellular uptake was also confirmed by increased SSC and intracellular silver content. In our previous study, the cytotoxic doses of HT22 cells to the uncoated AgNPs was 25–100 μg/mL [6], the difference of AgNPs could be caused by its coating on the surface. Coating with PVP could stabilize AgNPs in aqueous solution for a longer time than other silver nanomaterials [18]. Surface coating is only one of the influence factors for AgNPs. But it partly explains the toxic difference between the two kinds of AgNPs. Our results suggested acute exposure of AgNPs at low dose induced neurotoxicity in HT22 cells, which could provide a certain basis for subsequent experimental design.

Mitochondria are one of the main targets on nanoparticles-induced

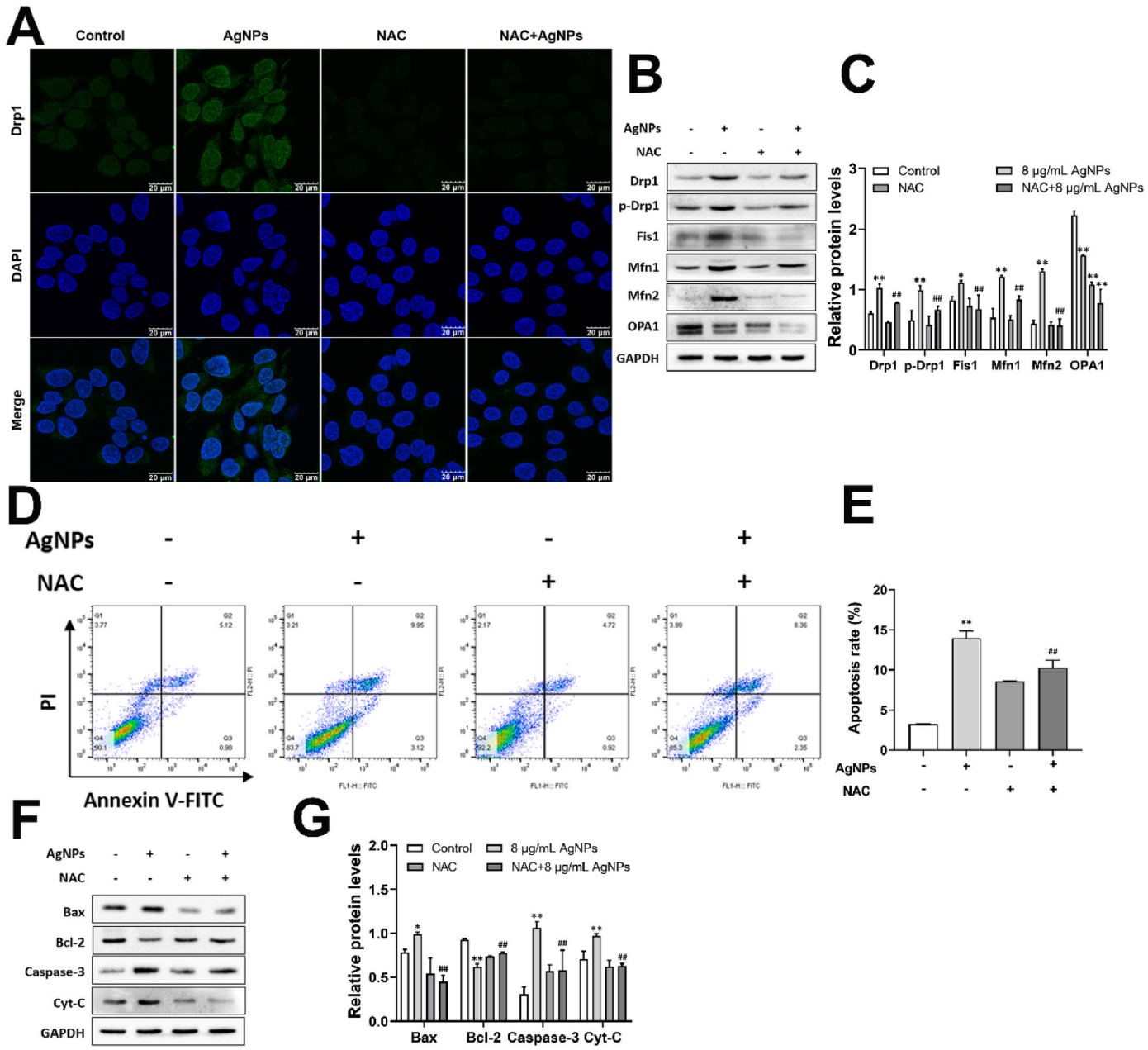

Fig. 7. ROS promoted mitochondrial fission/fusion and enhance mitochondria-dependent apoptosis induced by AgNPs in HT22 cells. HT22 cells were pretreated with/without NAC (5 mM) 2 h before exposure to 8 μg/mL AgNPs for 24 h. (A) Immunofluorescence of Drp1in HT22 cells; (B–C) Western blot for protein expression of Drp1, p-Drp1, Fis1, Mfn1, Mfn2, OPA1 in HT22 cells; (D–E) Apoptosis rate of HT22 cells; (F–G) Western blot for protein expression of Bax, Bcl-2, Caspase-3, Cyt-C in HT22 cells. Data are expressed as mean ± SD from three independent experiments. $^{*}p < 0.05$, $^{**}p < 0.01$ when compared with the control. $^{\#}p < 0.05$, $^{\#\#}p < 0.01$ when compared with the AgNPs (8 μg/mL) group.

cytotoxicity [17]. Mitochondrial structure and function are tightly linked, derangements are associated with cytotoxicity and profound physiological implications [19]. Our results showed that AgNPs (8 μg/mL) exposure for 24 h could significantly promote mitochondrial fission and induced mitochondrial fragmentation in HT22 cells. The toxicological responses of AgNPs on HT22 cells are consistent with recent studies on other different cell lines [4,14,20]. Mitochondrial morphological structures were damaged with AgNPs exposure in HT22 cells. Additionally, normal structure is essential for mitochondrial function. In our present study, short-term exposure to low-dose AgNPs caused an obvious mitochondrial dysfunction (increased ROS level and decreased MMP and ATP synthesis). It may be caused by mitochondrial structural alterations, characterized with mitochondrial fragmentation, cristae loss, vacuolation and even mitochondrial membrane rupture. The reduction in MMP and ATP caused by AgNPs was reversed by the removal of ROS, suggesting that ROS contributes to AgNPs-induced mitochondrial damage in hippocampal neurons. Furthermore, AgNPs-induced cytotoxicity focus on mitochondrial function, which has been implicated in cell death and neurodegeneration [20]. Despite mechanism of AgNPs-induced hippocampal neuronal mitochondrial fragments remain unclear, we considered ROS as a reason for mitochondrial damage via disturbance of mitochondrial dynamic.

Mitochondrial dynamic refers the dynamic maintenance of mitochondrial shape, length and quantity, which was driven by biomarkers of mitochondrial fission/fusion (including Drp1, Fis1, Mfn1, Mfn2 and OPA1) [4,21]. We further explore mitochondrial fission/fusion in ROS-promoted mitochondrial damage. Our study showed the increased protein expression in mitochondrial fission-related proteins Drp1 and

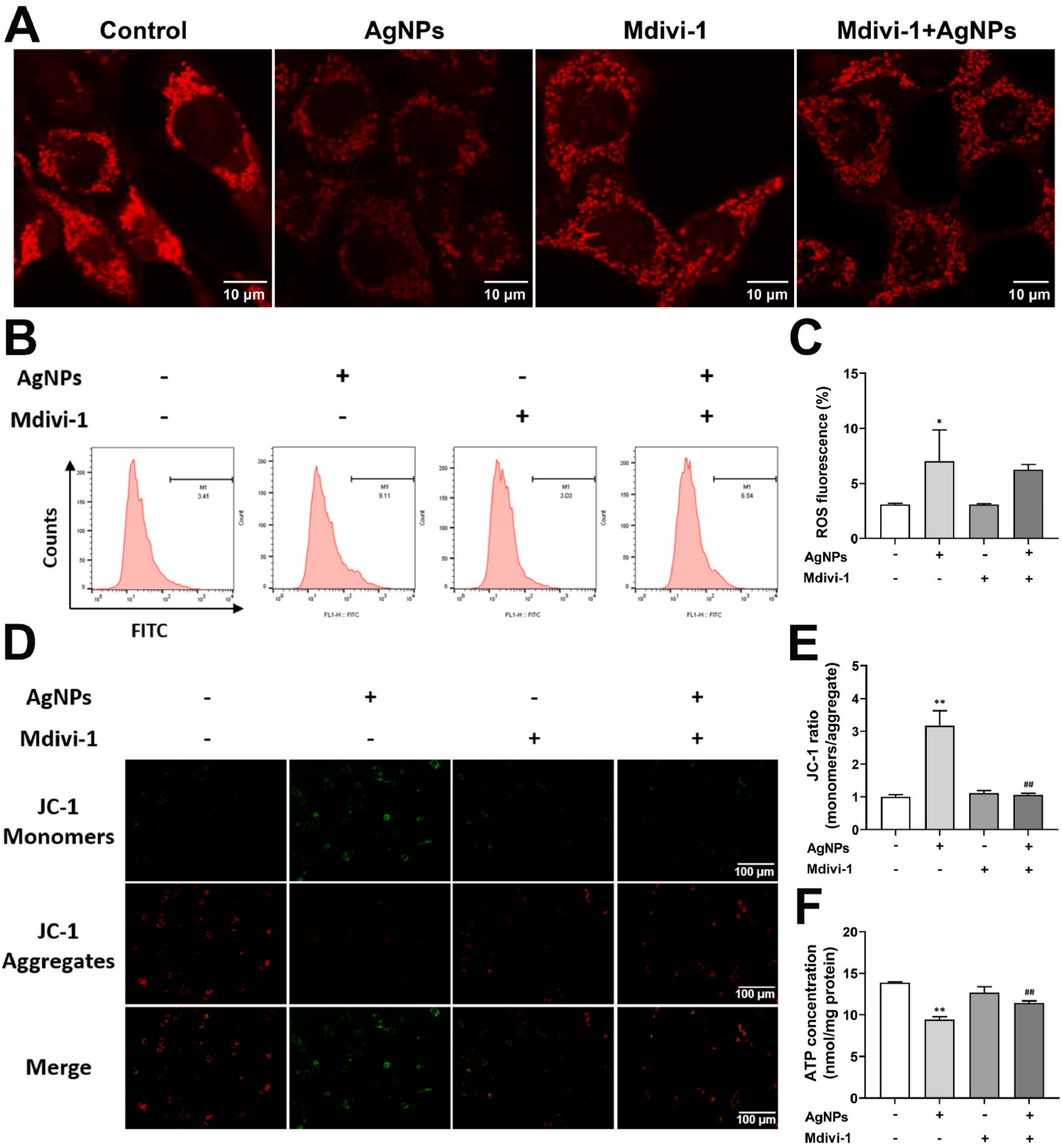

Fig. 8. Role of Drp1 on mitochondrial fragmentation and mitochondrial dysfunction induced by AgNPs in HT22 cells. HT22 cells were pretreated with/without Mdivi-1 (5 μM) 2 h before exposure to 8 μg/mL AgNPs for 24 h. (A) Alteration of Mitotracker fluorescence in HT22 cells; (B–C) Intracellular ROS levels in HT22 cells; (D–E) MMP changes in HT22 cells; (F) ATP content in HT22 cells. Data are expressed as mean ± SD from three independent experiments. $^{*}p < 0.05$, $^{**}p < 0.01$ when compared with the control. $^{\#}p < 0.05$, $^{\#\#}p < 0.01$ when compared with the AgNPs (8 μg/mL) group.

Fis1, and mitochondrial fusion-related proteins Mfn1 and Mfn2, while OPA1 protein expression was decreased by AgNPs in HT22 cells. Theses biomarkers were reversed by NAC except for OPA1 protein expression, indicating that ROS promoted mitochondrial fission and mitochondrial outer membrane fusion induced by AgNPs. Short round mitochondria were also reduced by NAC pretreatment. Our data indicated AgNPs-induced neurotoxicity, which was involved in mitochondrial fission and mitochondrial outer membrane fusion by ROS. Li et al. described the relationships among AgNPs exposure, ROS production, and mitochondrial fission in HepG2 cells, the finding is consistent with our results [13]. More importantly, phosphorylated Drp1 Ser616 expression was significantly increased by AgNPs in HT22 cells. Phosphorylation of Drp1 at Ser616 has been extensively studied [22], which could promote the translocation of Drp1 to mitochondria and initiate

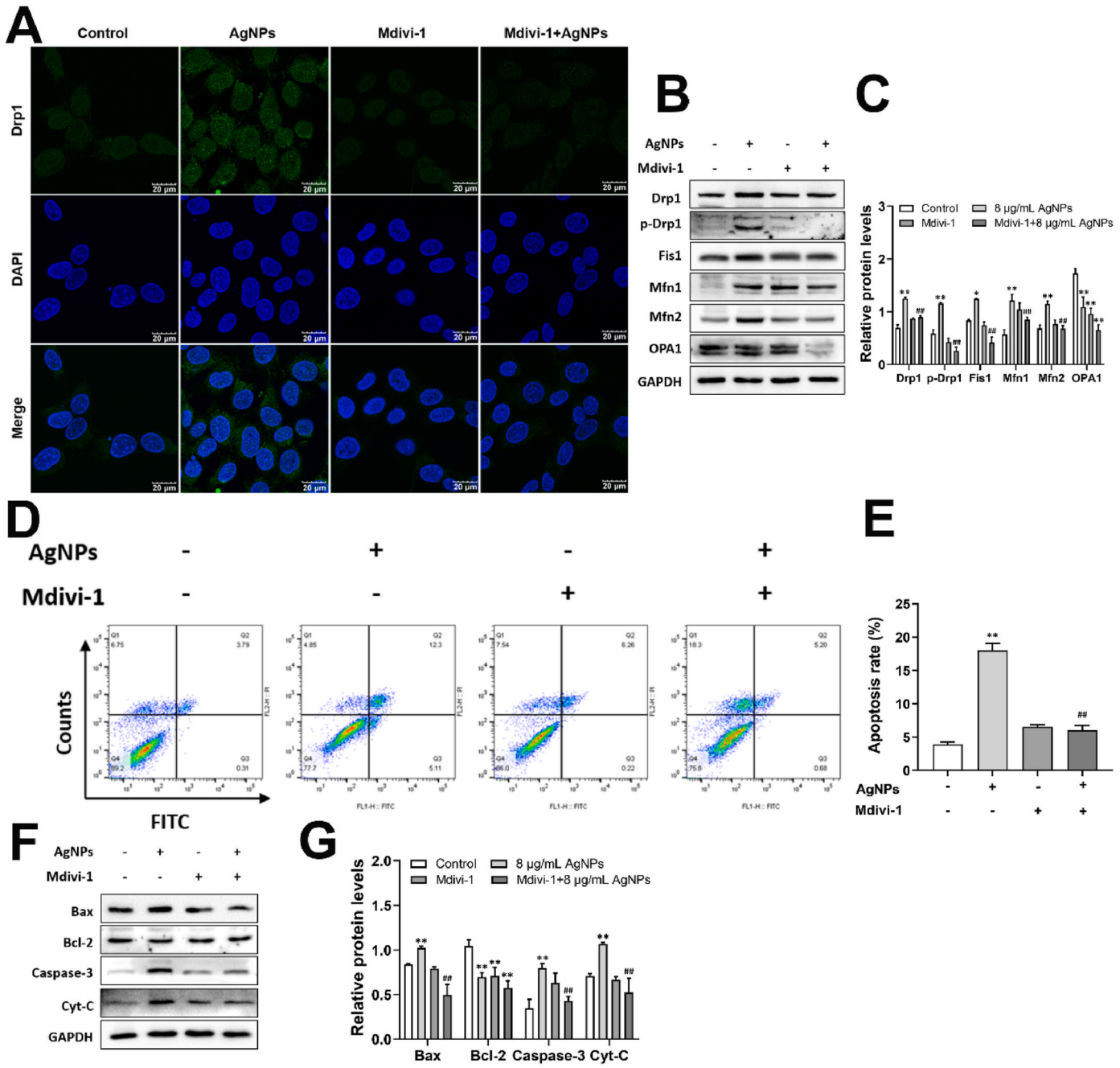

Fig. 9. Role of Drp1-mediated mitochondrial fission on apoptosis induced by AgNPs in HT22 cells. HT22 cells were pretreated with/without Mdivi-1 (5 μM) 2 h before exposure to 8 μg/mL AgNPs for 24 h. (A) Immunofluorescence of Drp1in HT22 cells; (B–C) Western blot for protein expression of Drp1, p-Drp1, Fis1, Mfn1, Mfn2, OPA1 in HT22 cells; (D–E) Apoptosis rate of HT22 cells; (F–G) Western blot for protein expression of Bax, Bcl-2, Caspase-3, Cyt-C in HT22 cells. Data are expressed as mean ± SD from three independent experiments. $^{*}p < 0.05$, $^{**}p < 0.01$ when compared with the control. $^{\#}p < 0.05$, $^{\#\#}p < 0.01$ when compared with the AgNPs (8 μg/mL) group.

mitochondria fission [23]. Drp1 regulates the dynamic balance of cell mitochondrial fission-fusion. Since Drp1-dependent fission signal is known to be an important pathway in toxic effect of nanoparticles [12], we pretreated HT22 cells with Mdivi-1 (Drp1 inhibitor). Our results showed that mitochondrial fission/fusion, mitochondrial fragment and dysfunction was partly rescued by Mdivi-1 pretreatment in AgNPs-cultured HT22 cells. But the Mdivi-1 pretreatment didn't inhibit the ROS generation caused by AgNPs, indicating the Drp1 is the downstream molecule of ROS. Increasing evidence demonstrates that mitochondrial function in mammals depends on Drp1-mediated mitochondrial fission [13,24–26]. But whether it has important role in AgNPs-induced neurotoxicity is controversial. Our results provide a new insight to study of ROS-Drp1-mitochndrial fission axis in neurotoxicity induced by AgNPs.

Nanoparticles-induced disturbance of mitochondrial fission/fusion is consequently to cause cell death (including apoptosis, necrosis and autophagy) [27]. A large number of researches have indicated potential associations between mitochondrial dynamic and apoptosis/inflammation with AgNPs/TiO_2 exposure in other target organs [20,28–30], but few literatures were found in AgNPs-induced neurotoxicity on this observation. Our present study suggested that AgNPs increased apoptotic ratio in HT22 cells. The intrinsic pathway of apoptosis is initiated by mitochondrial membrane permeabilization. ROS and mitochondrial dysfunction could further trigger apoptosis in

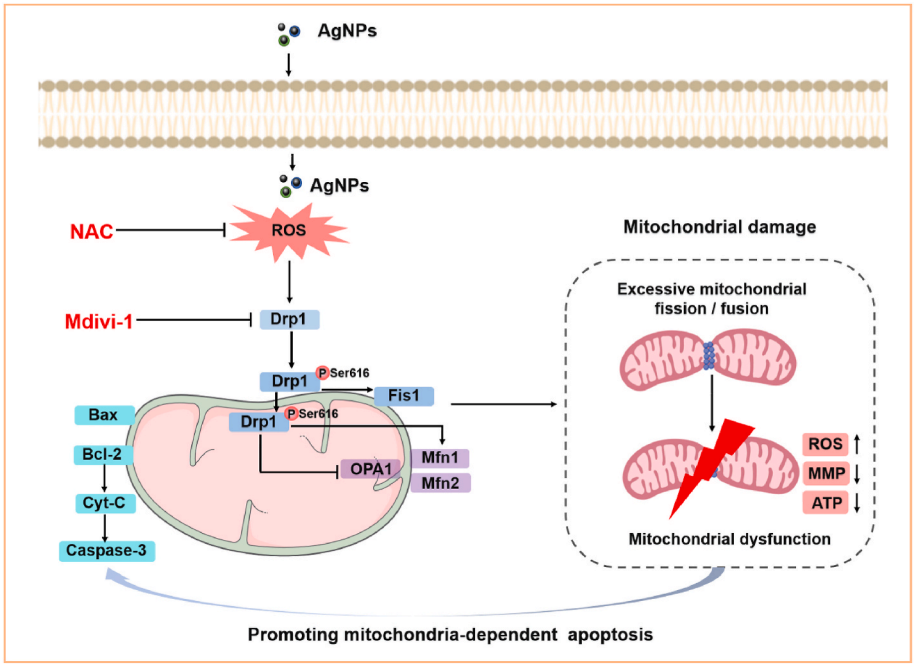

Fig. 10. Schematic diagram of signaling pathways involved in AgNPs-induced mitochondrial damage and apoptosis in hippocampal HT22 cells. AgNPs promoted mitochondrial fragmentation via excessive mitochondrial fission/fusion, increased ROS generation, decreased MMP and ATP synthesis, eventually induced mitochondria-dependent apoptosis in HT22 cells. The mechanism was involved in increased Drp1, Fis1, Mfn1, Mfn2 and decreased OPA1 expression, mainly mediated by phosphorylation and mitochondrial translocation of Drp1 Ser616. Furthermore, all aforementioned changes were significantly rescued by NAC and Mdivi-1 except for OPA1 expression, indicating that mechanism of mitochondria-dependent apoptosis in HT22 cells was mediated by excessive activation of ROS-Drp1-mitochondrial fission axis.

hippocampal neurons, which is supported by our previous study on AgNPs-induced HT22 cells apoptosis [6]. In this study, mitochondrial dysfunction and mitochondria-dependent apoptosis was also confirmed by increasing Bax, Caspase-3, Cyt-C expression and decreasing Bcl-2 expression caused by AgNPs in HT22 cells. Moreover, the increased apoptosis and involved biomarkers changes of HT22 cells caused by AgNPs was rescued by NAC and Mdivi-1, which is different with our previous study in HepG2 cells [13]. It may be attributed to the difference of cell type. Our findings revealed that mitochondrial damage was enrolled in AgNPs-induced neurotoxicity in HT22 cells. And ROS-Drp1-mitochondrial fission axis promoted the mitochondria-dependent apoptosis by acute exposure of AgNPs at low dose.

It remains unclear whether the cytotoxicity is due to the Ag^+ released from AgNPs themselves in AgNPs-induced neurotoxicity. In this study, the silver content was 0.095 ng/10^5 cells, and intracellular Ag^+ content was approximately 0.003 ng/10^5 cells in HT22 cells after AgNPs (8 μg/mL) exposure for 24 h. The results indicated that Ag^+ released from AgNPs in the HT22 cells was approximately 3.16%, and it is in line with our results in the cell uptake and AgNPs distribution confirmed by SSC detection and TEM observation. Moreover, for the mechanistic research, it was only AgNPs-treated HT22 cells that produced mitochondrial damage and mitochondrial-dependent apoptosis. Despite both AgNPs and Ag^+ caused cytotoxicity at different concentration, the mitochondrial fragment was only induced by AgNPs as well, which is consistent with our previous studies in HepG2 cells and A549 cells [4,21]. Zhang et al. also suggested that cytotoxicity in primary-cultured cortical neurons was owing to the AgNPs themselves [31]. These results supported our finding in this study, indicated that AgNPs-induced neurotoxicity is particle-specific AgNPs rather than silver ions release.

5. Conclusions

In conclusion, this study revealed that acute exposure to AgNPs at low dose induced mitochondrial damage and cytotoxicity in HT22 cells. AgNPs promoted the mitochondrial fragmentation and mitochondrial dysfunction (including ROS generation, ATP and MMP reduction), leading to mitochondria-dependent apoptosis. Moreover, ROS signaling and Drp1 regulation were found to have prominent impact on mitochondrial damage, and ROS-Drp1-mitochondrial fission axis promoted the mitochondria-dependent apoptosis in HT22 cells (Fig. 10). These findings contribute to our understanding of the toxic mechanisms underlying AgNPs-induced mitochondrial fission and apoptosis, imply that Drp1-mediated mitochondrial fission in hippocampal neurons could be an alternative target for the prevention and treatment of AgNPs-induced neurotoxicity.

Authorship statement

Xiaoru Chang: Conceptualization, Investigation, Data curation, Writing-original draft, Writing-review & editing, Project administration, Funding acquisition. Shuyan Niu, Mengting Shang, Jiangyan Li, Menghao Guo, Wenli Zhang, Zuoyi Sun, Yunjing Li, Rui Zhang, Xin Shen: Data curation. Meng Tang: Formal analysis, Project administration. Yuying, Xue: Writing-review & editing, Conceptualization, Project administration, Funding acquisition, Formal analysis.

Declaration of competing interest

The authors declare that they have no known competing financial interests or personal relationships that could have appeared to influence the work reported in this paper.

Data availability

Data will be made available on request.

Acknowledgment

This work was supported by National Natural Science Funds of China (82273674, 81573186), Postgraduate Research & Practice Innovation Program of Jiangsu Province (KYCX20_0152, KYCX21_0165).

Main abbreviations

AgNPs	silver nanoparticles
BAX	BCL2-associated X protein
BBB	blood brain barrier

BCL2	B-cell lymphoma-2
CCK8	cell counting kit 8
CNS	central nervous system
Cyt-C	cytochrome C
Drp1	GTPase dynamin-related protein 1
FF	form factor
Fis1	mitochondrial fission protein 1
ICP-MS	inductively coupled plasma mass spectrometry
Mfn1	mitofusin 1
Mfn2	mitofusin 2
MMP	mitochondrial membrane potential
NAC	N-acetyl-L-cysteine
OPA1	optic atrophy 1
PMSF	phenylmethanesulfonyl fluoride
PVP	polyvinylpyrrolidone
ROS	reactive oxygen species
TEM	transmission electron microscope

Appendix A. Supplementary data

Supplementary data to this article can be found online at https://doi.org/10.1016/j.redox.2023.102739.

References

[1] I.X. Yin, J. Zhang, I.S. Zhao, M.L. Mei, Q. Li, C.H. Chu, The antibacterial mechanism of silver nanoparticles and its application in dentistry, Int. J. Nanomed. 15 (2020) 2555–2562, https://doi.org/10.2147/IJN.S246764.

[2] Y. Li, E. Cummins, Hazard characterization of silver nanoparticles for human exposure routes, J. Environ. Sci. Health. A Tox. Hazard. Subst. Environ. Eng. 55 (2020) 704–725, https://doi.org/10.1080/10934529.2020.1735852.

[3] X. Chang, J. Li, S. Niu, Y. Xue, M. Tang, Neurotoxicity of metal-containing nanoparticles and implications in glial cells, J. Appl. Toxicol. 41 (2021) 65–81, https://doi.org/10.1002/jat.4037.

[4] J. Li, B. Zhang, X. Chang, J. Gan, W. Li, S. Niu, L. Kong, T. Wu, T. Zhang, M. Tang, Y. Xue, Silver nanoparticles modulate mitochondrial dynamics and biogenesis in HepG2 cells, Environ. Pollut. 256 (2020), 113430, https://doi.org/10.1016/j.envpol.2019.113430.

[5] L. Li, J. Cui, Z. Liu, X. Zhou, Z. Li, Y. Yu, Y. Jia, D. Zuo, Y. Wu, Silver nanoparticles induce sh-sy5y cell apoptosis via endoplasmic reticulum- and mitochondrial pathways that lengthen endoplasmic reticulum-mitochondria contact sites and alter inositol-3-phosphate receptor function, Toxicol. Lett. 285 (2018) 156–167, https://doi.org/10.1016/j.toxlet.2018.01.004.

[6] X. Chang, X. Wang, J. Li, M. Shang, S. Niu, W. Zhang, Y. Li, Z. Sun, J. Gan, W. Li, M. Tang, Y. Xue, Silver nanoparticles induced cytotoxicity in ht22 cells through autophagy and apoptosis via PI3K/AKT/mTOR signaling pathway, Ecotoxicol. Environ. Saf. 208 (2021), 111696, https://doi.org/10.1016/j.ecoenv.2020.111696.

[7] T. Yan, Y. Zhao, Acetaldehyde induces phosphorylation of dynamin-related protein 1 and mitochondrial dysfunction via elevating intracellular ros and Ca^{2+} levels, Redox Biol. 28 (2020), 101381, https://doi.org/10.1016/j.redox.2019.101381.

[8] Y. Qi, R. Ma, X. Li, S. Lv, X. Liu, A. Abulikemu, X. Zhao, Y. Li, C. Guo, Z. Sun, Disturbed mitochondrial quality control involved in hepatocytotoxicity induced by silica nanoparticles, Nanoscale 12 (2020) 13034–13045, https://doi.org/10.1039/d0nr01893g.

[9] R. Ning, Y. Shi, J. Jiang, S. Liang, Q. Xu, J. Duan, Z. Sun, Mitochondrial dysfunction drives persistent vascular fibrosis in rats after short-term exposure of PM2.5, Sci. Total Environ. 733 (2020), 139135, https://doi.org/10.1016/j.scitotenv.2020.139135.

[10] Y. Wang, L. Kong, T. Wu, M. Tang, Urban particulate matter disturbs the equilibrium of mitochondrial dynamics and biogenesis in human vascular endothelial cells, Environ. Pollut. 264 (2020), 114639, https://doi.org/10.1016/j.envpol.2020.114639.

[11] J. Jiang, S. Liang, J. Zhang, Z. Du, Q. Xu, J. Duan, Z. Sun, Melatonin ameliorates pm(2.5) -induced cardiac perivascular fibrosis through regulating mitochondrial redox homeostasis, J. Pineal Res. 70 (2021), e12686, https://doi.org/10.1111/jpi.12686.

[12] D. Wu, J. Lu, Y. Ma, Y. Cao, T. Zhang, Mitochondrial dynamics and mitophagy involved in mpa-capped cdte quantum dots-induced toxicity in the human liver carcinoma (HepG2) cell line, Environ. Pollut. 274 (2021), 115681, https://doi.org/10.1016/j.envpol.2020.115681.

[13] J. Li, X. Chang, M. Shang, S. Niu, W. Zhang, Y. Li, Z. Sun, T. Wu, L. Kong, T. Zhang, M. Tang, Y. Xue, The crosstalk between drp1-dependent mitochondrial fission and oxidative stress triggers hepatocyte apoptosis induced by silver nanoparticles, Nanoscale 13 (2021) 12356–12369, https://doi.org/10.1039/d1nr02153b.

[14] X. Chang, S. Niu, M. Shang, J. Li, W. Zhang, Z. Sun, Y. Li, T. Wu, T. Zhang, M. Tang, Y. Xue, Silver nanoparticles induced hippocampal neuronal damage involved in mitophagy, mitochondrial biogenesis and synaptic degeneration, Food Chem. Toxicol. 166 (2022), 113227, https://doi.org/10.1016/j.fct.2022.113227.

[15] Y. Sagara, D. Schubert, The activation of metabotropic glutamate receptors protects nerve cells from oxidative stress, J. Neurosci. 18 (1998) 6662–6671, https://doi.org/10.1523/JNEUROSCI.18-17-06662.1998.

[16] S.J. Yu, J.B. Chao, J. Sun, Y.G. Yin, J.F. Liu, G.B. Jiang, Quantification of the uptake of silver nanoparticles and ions to hepg2 cells, Environ. Sci. Technol. 47 (2013) 3268–3274, https://doi.org/10.1021/es304346p.

[17] D. Wu, Y. Ma, Y. Cao, T. Zhang, Mitochondrial toxicity of nanomaterials, Sci. Total Environ. 702 (2020), 134994, https://doi.org/10.1016/j.scitotenv.2019.134994.

[18] E. Topuz, L. Sigg, I. Talinli, A systematic evaluation of agglomeration of ag and tio 2 nanoparticles under freshwater relevant conditions, Environ. Pollut. 193 (2014) 37–44, https://doi.org/10.1016/j.envpol.2014.05.029.

[19] S. Yamada, D. Yamazaki, Y. Kanda, Silver nanoparticles inhibit neural induction in human induced pluripotent stem cells, Nanotoxicology 12 (2018) 836–846, https://doi.org/10.1080/17435390.2018.1481238.

[20] W. Ma, S. He, H. Ma, H. Jiang, N. Yan, L. Zhu, J.J. Bang, P.A. Li, S. Jia, Silver nanoparticle exposure causes pulmonary structural damage and mitochondrial dynamic imbalance in the rat: protective effects of sodium selenite, Int. J. Nanomed. 15 (2020) 633–645, https://doi.org/10.2147/IJN.S232986.

[21] J. Li, X. Chang, M. Shang, S. Niu, W. Zhang, B. Zhang, W. Huang, T. Wu, T. Zhang, M. Tang, Y. Xue, Mitophagy-lysosomal pathway is involved in silver nanoparticle-induced apoptosis in a549 cells, Ecotoxicol. Environ. Saf. 208 (2021), 111463, https://doi.org/10.1016/j.ecoenv.2020.111463.

[22] D. Lee, J. Min, H. Lee, D. Lee, Isoliquiritigenin attenuates glutamate-induced mitochondrial fission via calcineurin-mediated Drp1 dephosphorylation in HT22 hippocampal neuron cells, Neurotoxicology 68 (2018) 133–141, https://doi.org/10.1016/j.neuro.2018.07.011. Epub 2018 Jul 23.

[23] B. Ugarte-Uribe, C. Prévost, K.K. Das, P. Bassereau, A.J. García-Sáez, Drp1 polymerization stabilizes curved tubular membranes similar to those of constricted mitochondria, J. Cell Sci. 132 (2018), https://doi.org/10.1242/jcs.208603.

[24] X. Liu, X. Zhao, X. Li, S. Lv, R. Ma, Y. Qi, A. Abulikemu, H. Duan, C. Guo, Y. Li, Z. Sun, Pm(2.5) triggered apoptosis in lung epithelial cells through the mitochondrial apoptotic way mediated by a ros-drp1-mitochondrial fission axis, J. Hazard Mater. 397 (2020), 122608, https://doi.org/10.1016/j.jhazmat.2020.122608.

[25] S. Tang, S. Ye, Y. Ma, Y. Liang, N. Liang, F. Xiao, Clusterin alleviates cr(vi)-induced mitochondrial apoptosis in l02 hepatocytes via inhibition of Ca^{2+}-ROS-Drp1-mitochondrial fission axis, Ecotoxicol. Environ. Saf. 205 (2020), 111326, https://doi.org/10.1016/j.ecoenv.2020.111326.

[26] N. Chen, Z. Guo, Z. Luo, F. Zheng, W. Shao, G. Yu, P. Cai, S. Wu, H. Li, Drp1-mediated mitochondrial fission contributes to mitophagy in paraquat-induced neuronal cell damage, Environ. Pollut. 272 (2021), 116413, https://doi.org/10.1016/j.envpol.2020.116413.

[27] R. Mohammadinejad, M.A. Moosavi, S. Tavakol, D.Ö. Vardar, A. Hosseini, M. Rahmati, L. Dini, S. Hussain, A. Mandegary, D.J. Klionsky, Necrotic, apoptotic and autophagic cell fates triggered by nanoparticles, Autophagy 15 (2019) 4–33, https://doi.org/10.1080/15548627.2018.1509171.

[28] W. Ma, S. He, Y. Xu, G. Qi, H. Ma, J.J. Bang, P.A. Li, Ameliorative effect of sodium selenite on silver nanoparticles-induced myocardiocyte structural alterations in rats, Int. J. Nanomed. 15 (2020) 8281–8292, https://doi.org/10.2147/IJN.S271457.

[29] C.L. Wilson, V. Natarajan, S.L. Hayward, O. Khalimonchuk, S. Kidambi, Mitochondrial dysfunction and loss of glutamate uptake in primary astrocytes exposed to titanium dioxide nanoparticles, Nanoscale 7 (2015) 18477–18488, https://doi.org/10.1039/c5nr03646a.

[30] Q. Chen, N. Wang, M. Zhu, J. Lu, H. Zhong, X. Xue, S. Guo, M. Li, X. Wei, Y. Tao, H. Yin, Tio(2) nanoparticles cause mitochondrial dysfunction, activate inflammatory responses, and attenuate phagocytosis in macrophages: a proteomic and metabolomic insight, Redox Biol. 15 (2018) 266–276, https://doi.org/10.1016/j.redox.2017.12.011.

[31] B. Zhang, N. Liu, Q.S. Liu, J. Zhang, Q. Zhou, G. Jiang, Silver nanoparticles induce size-dependent and particle-specific neurotoxicity to primary cultures of rat cerebral cortical neurons, Ecotoxicol. Environ. Saf. 198 (2020), 110674, https://doi.org/10.1016/j.ecoenv.2020.110674.